



Climate variability effects on spatial soil moisture dynamics

Adriaan J. Teuling,¹ François Hupet,^{2,3} Remko Uijlenhoet,¹ and Peter A. Troch⁴

Received 28 December 2006; revised 14 February 2007; accepted 19 February 2007; published 24 March 2007.

[1] We investigate the role of interannual climate variability on spatial soil moisture variability dynamics for a field site in Louvain-la-Neuve, Belgium. Observations were made during 3 years under intermediate (1999), wet (2000), and extremely dry conditions (2003). Soil moisture variability dynamics are simulated with a comprehensive model for the period 1989–2003. The results show that climate variability induces non-uniqueness and two distinct hysteresis modes in the yearly relation between the spatial mean soil moisture and its variability. We demonstrate that the direction of hysteresis is related to a yearly climate index that does not require soil moisture observations. **Citation:** Teuling, A. J., F. Hupet, R. Uijlenhoet, and P. A. Troch (2007), Climate variability effects on spatial soil moisture dynamics, *Geophys. Res. Lett.*, 34, L06406, doi:10.1029/2006GL029080.

1. Introduction

[2] Soil moisture is an important variable in many land surface models since it controls the partitioning of fluxes of both water and energy. However soil moisture shows a large spatial variability, and the relation between soil moisture dynamics at a point (i.e., the scale of most observations) and that of a larger area (field, region) are still poorly understood. Over the past decades, field experiments have quantified the variability of soil moisture, its intra-seasonal dependence on the mean soil moisture state [Bell *et al.*, 1980; Famiglietti *et al.*, 1998], and its dependence on external factors such as soil, vegetation, and topography [e.g., Western *et al.*, 1999; Wilson *et al.*, 2004].

[3] Western *et al.* [2003, p. 130] analyzed spatial root zone soil moisture variability dynamics from 13 study areas around the globe (their Figure 8.6). Their analysis revealed that “variance increases with average moisture in dry catchments and it decreases in wet catchments. Where the spatial mean moisture has a sufficiently large range over time, the variance peaks at intermediate values.” While climate conditions are known to affect soil moisture variability dynamics [Teuling and Troch, 2005], little attention has been paid to the role of interannual climate variability on the dynamics of spatial soil moisture variability.

[4] Here we analyze the impact of both intra-annual climate dynamics and interannual climate variability on soil moisture variability at the field scale. We employ an

extension of the comprehensive soil moisture variability model by Teuling and Troch [2005]. The advantage of this approach is that the number of parameters (with generally unknown covariability) is small, while the parameters still reflect observable properties. Models of similar complexity have been shown to correctly simulate root zone soil moisture dynamics under different climatic conditions [Albertson and Kiely, 2001; Teuling *et al.*, 2005].

2. Method

2.1. Data

[5] Soil moisture variability was measured at multiple occasions during the growing seasons of 1999, 2000, and 2003 in a 1 ha agricultural field located in Louvain-la-Neuve, Belgium. The measurements were part of a campaign that aimed at investigating within-field variability of transpiration [Hupet and Vanclooster, 2002]. The same instruments were used, but in a different experimental setup (Figure 1). Detailed information on the 1999 and 2003 data can be found in works by Hupet and Vanclooster [2002] and Hupet and Vanclooster [2005], respectively. The 2000 data has not been analyzed before. The soils in the field can be classified as well-drained silty-loam and there is little relief. During the campaigns the field was cropped with maize (*Zea Mays* L.). The climate is temperate humid. Meteorological observations made in the vicinity of the field are available for the period 1 January 1989 until 28 August 2003.

2.2. Model

[6] We assume that the point-scale soil moisture dynamics are spatially unconnected. Vertical redistribution of soil moisture is assumed to occur instantaneously (at the daily time step). We solve the daily water balance for a number of independent soil columns of depth L :

$$\frac{d\theta}{dt} = \frac{1}{L}(T - S - E - R - q), \quad (1)$$

where θ is the volumetric soil moisture content, T the throughfall, S the root water uptake, E the evaporation from the soil surface, R the saturation excess runoff, and q the deep drainage. Here $L = 0.65$ m. Although roots can penetrate deeper than 0.65 m, most of the water uptake occurs above this depth. The number of columns is taken the same as the 1999 setup (28, Figure 1a). Throughfall is rainfall that is not intercepted by vegetation. The size of the interception reservoir is taken proportional to the leaf area index ξ (with a constant of 0.2 mm). Root water uptake is thought to be proportional to a maximum transpiration rate E_m , a soil moisture stress $\beta(\theta)$, and a function accounting for leaf area index following Al-Kaisi *et al.* [1989]:

$$S = \beta(\theta)E_m = \beta(\theta)[1 - \exp(-c\xi)]ET_0, \quad (2)$$

¹Hydrology and Quantitative Water Management Group, Wageningen University, Wageningen, Netherlands.

²Formerly at Department of Environmental Sciences and Land Use Planning, Université Catholique de Louvain, Louvain-la-Neuve, Belgium.

³Baxter Bioscience, Lessines, Belgium.

⁴Department of Hydrology and Water Resources, University of Arizona, Tucson, Arizona, USA.

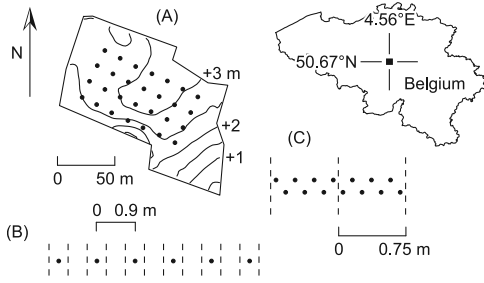


Figure 1. Location of the field and experimental setup: (a) 1999, with 0.5 m contour lines, (b) 2000 (detail of 45 m long transect), and (c) 2003, both with location of maize rows (dashed lines).

where c is a light use efficiency parameter (0.55), and ET_0 the potential evapotranspiration calculated by the FAO Penman-Monteith method [Allen *et al.*, 1998]. The positive relation between ξ and S was confirmed by Hupet and Vanclooster [2004]. Soil moisture stress is modeled as:

$$\beta(\theta) = \begin{cases} 0, & \theta \leq \theta_w \\ \frac{\theta - \theta_w}{\theta_c - \theta_w}, & \theta_w < \theta \leq \theta_c \\ 1, & \theta_c < \theta \leq \theta_s, \end{cases} \quad (3)$$

where the critical moisture content θ_c defines the transition between unstressed and stressed transpiration, θ_s is the porosity, and the wilting point θ_w corresponds to a pressure head of -150 m. To account for the effect of different E_m on θ_c [e.g., Denmead and Shaw 1962], we determine θ_c dynamically from $(\theta_c - \theta_w)/(\theta_f - \theta_w) = E_m/E_s$, where θ_f is the field capacity and $E_s = 10 \text{ mm d}^{-1}$ the maximum sustainable uptake at θ_f . The field capacity corresponds to a hydraulic conductivity k of 1 mm d^{-1} and is derived from:

$$k(\theta) = k_s \left(\frac{\theta}{\theta_s} \right)^{2b+3}, \quad (4)$$

where k_s is the value of k at saturation and b a pore size distribution parameter. We assume E to be proportional to the remaining fraction bare soil ($\exp(-c\xi)$), ET_0 , and the inverse of the square root of time since the last rainfall event ($\geq 10 \text{ mm}$). E is included for a correct water balance when ξ is small, but it has little effect on the soil moisture variability. Leaf area index ξ is modeled as:

$$\xi(t) = \begin{cases} 0, & t \leq t_s \\ \frac{\xi_{\max}}{2} \left[1 - 1 \cos\left(2\pi \frac{t-t_s}{t_d}\right) \right], & t_s < t \leq t_h \\ 0, & t > t_h, \end{cases} \quad (5)$$

where the sowing and harvest days t_s and t_h are taken as 119 and 283, respectively, and $t_d = 260$ for all years. This implies that both the dynamics and variability of ξ are considered to be the same for all years. Runoff R is the part of T that causes oversaturation of the soil. Drainage q is assumed to be driven only by gravity, i.e., $k = q$ with $k(\theta)$ defined by (4).

[7] The spatial distribution of ξ_{\max} is assumed to be normal, with mean 3.6 and standard deviation 0.5 derived from observations [Hupet and Vanclooster, 2002]. The

spatial distribution of $\ln(k_s)$ is also assumed to be normal, with parameters 5.6 and 0.4 fitted from observed k_s at the site. As in the work by Teuling and Troch [2005], we relate θ_s and b to k_s by regressions derived from the data of Clapp and Hornberger [1978]. These are $\theta_s = -0.0147 \ln(k_s) + 0.545$ and $b = -1.24 \ln(k_s) + 15.3$. Since soil and vegetation properties can show spatial correlation, we need to specify the (linear) correlation coefficient of the joint spatial distribution of $\ln(k_s)$ and ξ_{\max} . Due to the positive effect of high k_s on canopy growth through better aeration, soil temperature and water transport to roots, we assume a positive correlation of 0.8. Impacts of correlation between soil and vegetation fields are discussed by Montaldo and Albertson [2003]. For every year, the soil moisture field was initialized at θ_f .

2.3. Analysis

[8] It is of interest to identify the processes that are responsible for the temporal changes in spatial variability of the simulated soil moisture field (here expressed as a variance σ_s^2 or standard deviation σ_s). Albertson and Montaldo [2003] showed how the temporal changes in σ_s^2 are related to the covariances of the different water balance terms and the soil moisture field. For our water balance (1) this yields:

$$\frac{d\sigma_s^2}{dt} = \underbrace{\frac{2}{L} (\overline{\theta' T'} - \overline{\theta' E'} - \overline{\theta' S'})}_{\text{Vegetation}} - \underbrace{\frac{2}{L} (\overline{\theta' R'} + \overline{\theta' q'})}_{\text{Soil}}, \quad (6)$$

where the horizontal bars indicate spatial averaging, and the prime a deviation from the spatial average. For convenience, the different terms in (6) have been grouped by vegetation and soil effects on $d\sigma_s^2/dt$. E is listed in the vegetation group since in our model it depends on ξ rather than soil characteristics.

[9] An important variable that characterizes soil moisture dynamics in (sub)humid areas is Ψ [Teuling *et al.*, 2005]. It is defined as the maximum precipitation deficit during the growing season (D_P , calculated with respect to E_m) and scaled by the storage available for “unstressed” plant uptake:

$$\Psi = \frac{D_P}{L(\overline{\theta_f} - \overline{\theta_c})}, \quad (7)$$

where $\overline{\theta_c}$ is taken at $E_m = 3 \text{ mm d}^{-1}$. Ψ not only depends on climate (through D_P), but also on soil and vegetation characteristics. Deeper rooting vegetation will have lower Ψ , but also a more damped soil moisture dynamics. Teuling *et al.* [2005] showed that the expected value of this index can explain differences in observed soil moisture dynamics. Here we determine Ψ for each year separately.

3. Results

3.1. Observations

[10] The upper panels in Figure 2 show the observed soil moisture variability dynamics for the root zone ($\sim 0.65 \text{ m}$). Although the observations were made at different spatial scales (Figure 1), we argue that the effect of spatial scale is reflected in the magnitude of σ_o rather than in its trend. In 1999, σ_o showed an increasing trend with decreasing $\overline{\theta}$, while during the extremely dry summer of 2003, a similar

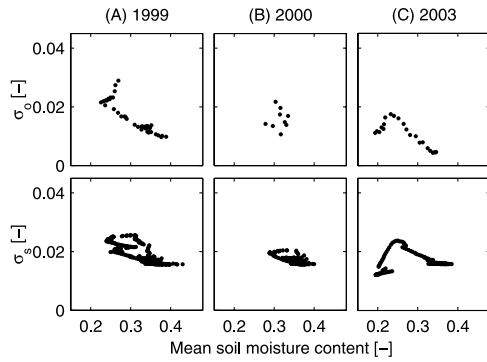


Figure 2. Observed (σ_o) and simulated (σ_s) soil moisture variability versus spatial mean soil moisture ($\bar{\theta}$) for the years 1999, 2000, and 2003.

initial increase in σ_o was followed by a strong decrease at low $\bar{\theta}$. In 2000, neither $\bar{\theta}$ nor σ_o showed strong dynamics. A more comprehensive analysis of soil moisture variability in the years 1999 and 2003 can be found in the work by *Hupet and Vanclooster* [2002] and *Hupet and Vanclooster* [2005], respectively. Since the observations are limited in extent (namely 3 growing seasons) and temporal resolution, they show only partly the hysteresis associated with rapid rewetting after rainfall. This is further investigated using simulations.

3.2. Simulations

[11] The lower panels in Figure 2 show the relation between the simulated mean soil moisture and its standard deviation σ_s . Note that in contrast to the observations, the simulations for the different years apply to the same spatial scale, and are not limited to the growing season. An important element of the simulated soil moisture field is that its variability near $\bar{\theta}_f$ is nearly constant. This is the soil “footprint”, which corresponds to the variability that accommodates a spatially uniform q . For all three years, the simulations show behavior similar to the observations. Both the range in $\bar{\theta}$ and the different trends in σ_o are realistically simulated. While the observations do not cover the rewetting to $\bar{\theta}_f$ after the growing season, the simulations reveal that the relation between $\bar{\theta}$ and σ_s does not only show different trends, but is also subject to hysteresis. Interestingly, the direction of this hysteresis can vary.

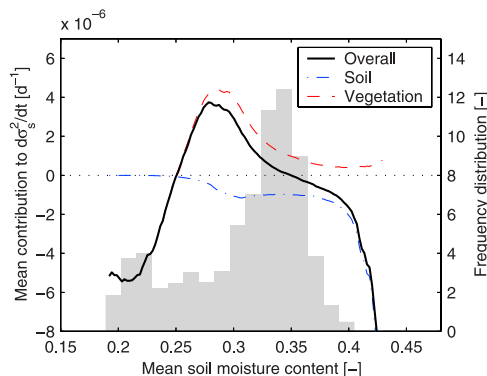


Figure 3. Dependence of the vegetation and soil contributions to $d\sigma_s^2/dt$ on mean soil moisture $\bar{\theta}$, and frequency distribution of $\bar{\theta}$ for the growing season (1989–2003).

[12] First we focus on the question what causes the non-uniqueness in the relation between $\bar{\theta}$ and σ_s . Figure 3 shows the average vegetation and soil contributions to the variance rate of change budget in (6) as a function of $\bar{\theta}$. It should be noted that the soil and vegetation groups are dominated by $\bar{\theta}q'$ and $\bar{\theta}'S'$, respectively. There is a clear structure in the vegetation contributions to $d\sigma_s^2/dt$. If $\bar{\theta}$ is above ~ 0.25 , then the spatial variability in S (which for $\theta \geq \theta_c$ is not sensitive to soil moisture) causes σ_s to increase. The spatial variability in S is due to the spatial variability in leaf area index. At lower $\bar{\theta}$, the vegetation contributions switch sign (S becomes a strong function of θ) and their magnitude increases. This can be explained by the fact that when soil moisture is limiting, roots take up more water in wet soil columns than in dry ones. By doing so, they decrease the spatial (inter-column) variability.

[13] The transition between these two states is relatively fast, as is indicated by the corresponding local minimum at 0.25 in the bimodal frequency distribution of $\bar{\theta}$. Soil contributions are only significant near $\bar{\theta}_f$ (~ 0.35), and counteract the vegetation effects ($d\sigma_s^2/dt \approx 0$). Vegetation effects are limited to the growing season. Negative vegetation contributions do not occur early in the growing season when $\bar{\theta}$ is high. In this period, the counteracting effect of the soil contributions is also highest. Occasional positive soil contributions occur directly after the end of the growing season. Figure 3 also shows that $d\sigma_s^2/dt$ converges to the vegetation or soil contributions in the dry or wet soil moisture range, respectively. This confirms the strong dependency of the different soil moisture variability controls on $\bar{\theta}$.

[14] The different trends in σ_s (increasing or increasing followed by decreasing) with decreasing spatial mean soil moisture lead to different hysteresis loops in the relation between $\bar{\theta}$ and σ_s , since the soil contributions that counteract the previous vegetation effects on σ_s become significant only once the soil is rewetted to near $\bar{\theta}_f$ (Figure 3). This is illustrated in Figure 4 for the years 1989 (dry) and 2002 (wet). The bimodal growing season soil moisture frequency distribution in 1989 illustrates that during a large part of the season, $\bar{\theta}$ is below $\bar{\theta}_c$, and vegetation destroys spatial variance. This does not occur in 2002, when the distribution is unimodal. This shows that $\bar{\theta}_c$ acts as a threshold that controls soil moisture variability dynamics. The yearly climate index Ψ , which does not require information on soil moisture status, is a good predictor for the crossing of the threshold. Figure 5 confirms that low Ψ (<1) is associated with clockwise hysteresis in the relation between $\bar{\theta}$ and

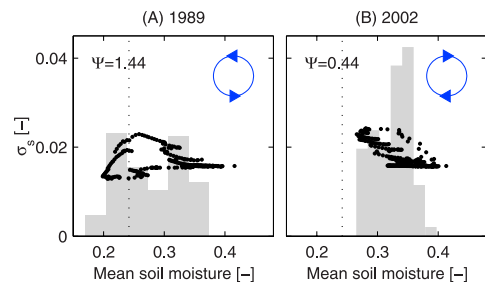


Figure 4. Relation between $\bar{\theta}$ and σ_s and direction of hysteresis for the years 1989 and 2002. The grey area indicates the corresponding frequency distribution of $\bar{\theta}$ for the growing season, and dotted line $\bar{\theta}_c$ for $E_m = 3 \text{ mm d}^{-1}$.

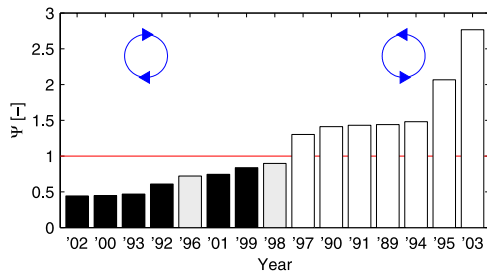


Figure 5. Index Ψ for the 15 years of simulation, sorted in increasing order. Small values ($\Psi < 1$) result in clockwise hysteresis (black), while large values ($\Psi > 1$) result in anti-clockwise hysteresis (white). Years in grey have no clear hysteresis direction.

σ_{ss} , and high $\Psi (>1)$ with anti-clockwise hysteresis. Note that the crossing not necessarily occurs exactly at $\Psi = 1$, due to variability in θ_c and the initial soil moisture content at the start of the period over which D_P is determined.

4. Discussion and Conclusions

[15] This research highlights the role of climate variability on the spatial soil moisture dynamics. We conclude the following:

[16] 1. The yearly relation between spatial mean soil moisture and its standard deviation is non-unique.

[17] 2. The yearly relation between spatial mean soil moisture and its standard deviation is subject to hysteresis. The direction of hysteresis in time is clockwise for relatively wet years, and anti-clockwise for dry years. Starting from field capacity, both types of hysteresis loops share a similar initial increase in standard deviation with decreasing mean soil moisture.

[18] The dynamic nature of soil moisture variability has important implications for current approaches to aggregation and scaling of soil moisture. For instance, the fact that vegetation effects on soil moisture fields are affected by climate variability might explain observed differences in scaling of surface soil moisture fields for the same region during different field campaigns [Oldak et al., 2002]. Furthermore in many aggregation studies, soil moisture variability is assumed to be constant or to be uniquely related to mean soil moisture. These assumptions might not be appropriate.

[19] In this study we prescribe the seasonal development of leaf area index rather than to model its development dynamically in response to atmospheric and soil moisture conditions. Our reasons for doing so are twofold: a) we could not validate its interannual variability, and b) we had no information on the processes that caused its observed spatial variability. Although including vegetation dynamics might affect the interannual variability of soil moisture, we assume these effects to be small for the vegetation and climate at Louvain-la-Neuve.

[20] While spatial patterns of soil moisture might primarily reflect patterns in soil and vegetation, this research shows that climate variability effects on the temporal dynamics of the soil moisture field (which mainly occur through uptake by vegetation) cannot be neglected. Different hysteresis loops in the relation between mean soil

moisture and its variability might be a general feature of soil moisture variability dynamics in many other regions. Future research has to reveal if this is indeed the case.

[21] **Acknowledgments.** This research is supported by the Wageningen Institute for Environment and Climate Research (WIMEK), the research programme Climate Change of Wageningen University and Research Center, and the project Development of a European Land Data Assimilation System to predict Floods and Droughts (ELDAS, EVG1-CT-2001-00050). R.U. acknowledges financial support from the Netherlands Organization for Scientific Research (NWO) through a Innovational Research Incentives Scheme grant (project 016.021.003).

References

- Albertson, J. D., and G. Kiely (2001), On the structure of soil moisture time series in the context of land surface models, *J. Hydrol.*, *243*, 101–119.
- Albertson, J. D., and N. Montaldo (2003), Temporal dynamics of soil moisture variability: 1. Theoretical basis, *Water Resour. Res.*, *39*(10), 1274, doi:10.1029/2002WR001616.
- Al-Kaisi, M., L. J. Brun, and J. W. Enz (1989), Transpiration and evapotranspiration from maize as related to leaf area index, *Agric. For. Meteorol.*, *48*, 111–116.
- Allen, R. G., Pereira, L. S., D. Raes, and M. Smith (1998), Crop evapotranspiration, *FAO Irrig. Drain. Pap. 56*, Food and Agric. Organ., Rome.
- Bell, K. R., B. J. Blanchard, T. J. Schmutge, and M. W. Witzak (1980), Analysis of surface moisture variations within large-field sites, *Water Resour. Res.*, *16*(4), 796–810.
- Clapp, R. B., and G. M. Hornberger (1978), Empirical equations for some soil hydraulic properties, *Water Resour. Res.*, *14*(4), 601–604.
- Denmead, O. T., and R. H. Shaw (1962), Availability of soil water to plants as affected by soil moisture content and meteorological conditions, *Agron. J.*, *54*, 385–390.
- Famiglietti, J. S., J. W. Rudnicki, and M. Rodell (1998), Variability in surface moisture content along a hillslope transect: Rattlesnake Hill, Texas, *J. Hydrol.*, *210*, 259–281.
- Hupet, F., and M. Vanclooster (2002), Intraseasonal dynamics of soil moisture variability within a small agricultural maize cropped field, *J. Hydrol.*, *261*, 86–101.
- Hupet, F., and M. Vanclooster (2004), Sampling strategies to estimate field areal evapotranspiration fluxes with a soil water balance approach, *J. Hydrol.*, *292*, 262–280, doi:10.1016/j.jhydrol.2004.01.006.
- Hupet, F., and M. Vanclooster (2005), Micro-variability of hydrological processes at the maize row scale: Implications for soil water content measurements and evapotranspiration estimates, *J. Hydrol.*, *303*, 247–270, doi:10.1016/j.jhydrol.2004.07.017.
- Montaldo, N., and J. D. Albertson (2003), Temporal dynamics of soil moisture variability: 2. Implications for land surface models, *Water Resour. Res.*, *39*(10), 1275, doi:10.1029/2002WR001618.
- Oldak, A., Y. Pachepsky, T. J. Jackson, and W. J. Rawls (2002), Statistical properties of soil moisture images revisited, *J. Hydrol.*, *255*, 12–24.
- Teuling, A. J., and P. A. Troch (2005), Improved understanding of soil moisture variability dynamics, *Geophys. Res. Lett.*, *32*, L05404, doi:10.1029/2004GL021935.
- Teuling, A. J., R. Uijlenhoet, and P. A. Troch (2005), On bimodality in warm season soil moisture observations, *Geophys. Res. Lett.*, *32*, L13402, doi:10.1029/2005GL023223.
- Western, A. W., R. B. Grayson, G. Blöschl, G. R. Willgoose, and T. A. McMahon (1999), Observed spatial organization of soil moisture and its relation to terrain indices, *Water Resour. Res.*, *35*(3), 797–810.
- Western, A. W., R. B. Grayson, G. Blöschl, and D. J. Wilson (2003), Spatial variability of soil moisture and its implications for scaling, in *Scaling Methods in Soil Physics*, edited by Y. Perchepsky, M. Selim, and D. Radcliffe, chap. 8, pp. 119–142, CRC Press, Boca Raton, Fla.
- Wilson, D. J., A. W. Western, and R. B. Grayson (2004), Identifying and quantifying sources of variability in temporal and spatial soil moisture observations, *Water Resour. Res.*, *40*, W02507, doi:10.1029/2003WR002306.

F. Hupet, Baxter Bioscience, Blvd René Branquart, 80, B-7860 Lessines, Belgium.

A. J. Teuling and R. Uijlenhoet, Hydrology and Quantitative Water Management Group, Wageningen University, Droevendaalsesteeg 4, Atlas building (104), P.O. Box 47, NL-6700 AA, Wageningen, Netherlands. (ryan.teuling@wur.nl)

P. A. Troch, Department of Hydrology and Water Resources, University of Arizona, 1133 E. James E. Rogers Way, P.O. Box 210011, Tucson, AZ 85721, USA.